Toward engineering functional organ modules by additive manufacturing

2012 Biofabrication 4 022001

(http://iopscience.iop.org/1758-5090/4/2/022001)

Biofabrication **4** (2012) 022001 (12pp) doi:10.1088/1758-5082/4/2/022001

TOPICAL REVIEW

Toward engineering functional organ modules by additive manufacturing

Francoise Marga[1], Karoly Jakab[1], Chirag Khatiwala[2], Benjamin Shepherd[2], Scott Dorfman[2], Bradley Hubbard[3], Stephen Colbert[3] and Gabor Forgacs[1,2,4,5,6]

[1] Department of Physics and Astronomy, University of Missouri, Columbia, MO 65211, USA
[2] Organovo, Inc., 5871 Oberlin Drive, San Diego, CA 92121, USA
[3] Department of Plastic Surgery, University of Missouri, Columbia, MO 65211, USA
[4] Department of Biomedical Engineering, University of Missouri, Columbia, MO 65211, USA
[5] The Shipley Center for Innovation, Clarkson University, Potsdam, NY 13699, USA

E-mail: forgacsg@missouri.edu

Received 7 December 2011
Accepted for publication 17 January 2012
Published 12 March 2012
Online at stacks.iop.org/BF/4/022001

Abstract
Tissue engineering is emerging as a possible alternative to methods aimed at alleviating the growing demand for replacement tissues and organs. A major pillar of most tissue engineering approaches is the scaffold, a biocompatible network of synthetic or natural polymers, which serves as an extracellular matrix mimic for cells. When the scaffold is seeded with cells it is supposed to provide the appropriate biomechanical and biochemical conditions for cell proliferation and eventual tissue formation. Numerous approaches have been used to fabricate scaffolds with ever-growing complexity. Recently, novel approaches have been pursued that do not rely on artificial scaffolds. The most promising ones utilize matrices of decellularized organs or methods based on multicellular self-assembly, such as sheet-based and bioprinting-based technologies. We briefly overview some of the scaffold-free approaches and detail one that employs biological self-assembly and bioprinting. We describe the technology and its specific applications to engineer vascular and nerve grafts.

(Some figures may appear in colour only in the online journal)

Abbreviations

ECM	extracellular matrix
CVD	cardiovascular disease
HASMC	human aortic smooth muscle cell
HAEC	human aortic endothelial cell
HDFb	human dermal fibroblast
ID	inner diameter
DAH	differential adhesion hypothesis
SC	Schwann cells
PLGA	polylactic glycolic acid
BMSC	bone marrow stem cell
MSC	mesenchymal stem cell

[6] Author to whom any correspondence should be addressed.

1. Introduction

The classical tissue engineering paradigm [1] is to seed and grow cells in biocompatible matrix materials—scaffolds—designed to direct cell differentiation and functional assembly into three-dimensional tissues [2]. To mimic the *in vivo* milieu, the developing tissue is cultured in a bioreactor providing the necessary molecular and physical signals [3], followed by implantation into the host, where further maturation and integration are anticipated.

Scaffolds have been fabricated from both synthetic and natural polymers and used to engineer tissue grafts of great variety (e.g. skin, cartilage, bone, blood vessels, skeletal muscle, bladder, trachea, myocardium [4–8]). To be useful for tissue engineering, these polymers must be biodegradable, have an architecture compatible with cell type, size, nutrient transport to maintain viability and growth. They have to be engineered to assure that their degradation rate matches the rate at which cells within them deposit their own cell and tissue-specific extracellular matrix (ECM). Scaffolds often need to contain soluble clues (e.g. growth factors, morphogens) and are assembled to slowly release them [9, 10] or shaped according to the geometry of the desired construct [11, 12]. Despite these limiting conditions, scaffold-based tissue engineering has led to some spectacular clinically relevant results [11, 13–18]. Due to the many challenges for scaffolds, alternative approaches have appeared recently. One is based on decellularized native ECMs, and the other exploits the innate properties of cells to produce their own ECM (i.e. scaffold-free tissue engineering).

The use of the decellularized, tissue-specific ECM eliminates a number of difficulties associated with scaffold-based tissue engineering [19–21]. The method is based on removing the cellular and nuclear content of xenogenic or homogenic organs and reseeding the resulting tissue or the organ-specific ECM with the recipient's cells [22–30]. This approach has led to spectacular results in tissue and full organ reconstruction, such as cardiovascular repair [31], readily available vascular grafts for hemodialysis access [32], complete bioartificial heart [33], vascularized liver organoid [34] and clinical restoration of dysfunctional airway [35]. To ensure that no immunogenic reaction is triggered by the decellularized ECM, it is vital to remove all cellular material. The efficiency of removal depends on the origin of the tissue or organ. Thus the specific chemical and enzymatic methods of decellularization must be selected with great care [20, 31]. Furthermore, when the decellularized matrices of complex heterogeneous organs (e.g. heart) are repopulated with various cell types it is not obvious how to determine their ratio.

Fully biological tissue engineering is free of exogenous scaffolds. Instead, it is based on cellular self-assembly that relies, among others, on the ability of cells to develop their own tissue-specific ECM. In one approach, sheets of cells are engineered and cultured until they develop the ECM. Sheets wrapped into tubes have been used to build fully biological nerve grafts [36] and autologous vascular grafts [37, 38] with promising functional results in early human clinical trials [38–40]. Combining sheets gives rise to three-dimensional tissues with complex architecture [41], which can be used for cell-based therapy [42].

Another self-assembly-based approach detailed in this work is based on the recognition that 'nature knows best'. Here, a multicellular assembly, with composition dictated by the tissue or organoid to be engineered, is prepared in an initial configuration compatible with the topology of that tissue or organ. It then self-assembles through morphogenetic processes akin to those in early development, into the desired three-dimensional structure [43]. In the technology discussed here, the initial configuration of the multicellular system is prepared by the automated deposition of bioink particles (conveniently prepared multicellular aggregates) and a biocompatible temporary support, using specialized delivery devices [44, 45].

Several types of delivery methods exist for such solid free-form fabrication of cellular constructs: inkjet bioprinters (desktop inkjet printers redesigned and enabled to deliver cells also in the vertical direction) [46–50], direct cell writing using pneumatically powered nozzle systems [51] or laser guidance [52–54] and mechanical extruders [55, 56].

Fully biological, self-assembly-based tissue engineering, in particular when combined with additive manufacturing methods, has the potential to deliver constructs that resemble most their *in vivo* counterparts both architecturally and functionally. The disadvantage of the method is that the development of the natural ECM is time consuming and *in vitro* self-assembly may differ from that under fully physiological conditions. Finally, as with all tissue engineering approaches, the regulatory hurdles will be substantial.

Below we overview a particular scaffold-free, self-assembly-based approach that utilizes bioprinting, and discuss two specific applications: the engineering of vascular and nerve grafts.

2. Self-assembly-based tissue engineering by bioprinting

The major components of the print-based tissue engineering technology detailed below are the bioink, the temporary support structure and the bioprinter.

2.1. Bioink

The bioink particles are multicellular aggregates (spheroids or cylinders) composed of cell types consistent with the tissue or organ structure to be printed. These can be prepared in multiple ways [57]. As for printing ideally they have to be of consistent size, we have developed a specific method of preparation (for details see [58]). Cells are cultured under usual conditions in a cell-type specific medium in Petri dishes or standard culture flasks, transferred to 10 ml tissue culture flasks, incubated and centrifuged. Resulting pellets are aspirated into special-purpose micropipettes, 250–500 μm in diameter, incubated to re-establish cell–cell adhesive contacts and extruded. For spherical bioink, extruded cylinders are cut into equal fragments that are let to round up overnight on a gyratory shaker. Depending on the diameter of the micropipette, this procedure provides spheroids of a defined size and cell number (typically several thousand cells; figure 1(*A*)). For cylindrical bioink, cylinders are extruded by the bioprinter into specifically prepared cell-inert hydrogel molds (figures 1(*B*) and (*C*)) for overnight maturation. The spherical or cylindrical bioink units are finally aspirated into micropipettes, which serve as printer cartridges (figure 2(*A*)).

2.2. Support structure and bioprinter

Cartridges are loaded into the printer (figure 2(*B*)), which deposits the bioink particles and support structure according

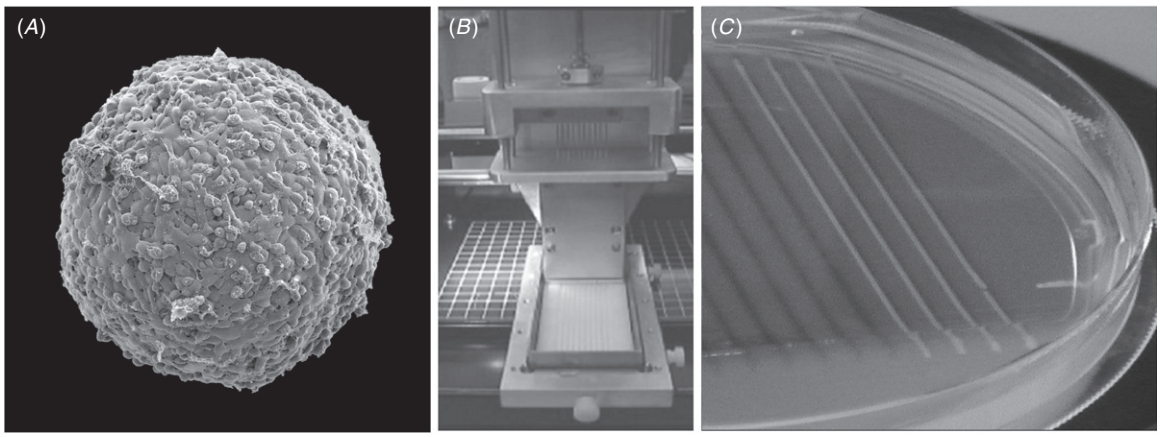

Figure 1. (*A*) Scanning electron microscopy image of a 500 μm diameter spherical cell aggregate composed of Chinese hamster ovary cells. (*B*) Multichannel extrusion device mounted on a bioprinter. (*C*) Simultaneous extrusion of multicellular cylinders into a non-adhesive agarose mold. (Figure reproduced from [58].)

to a specific design template. The support structure, typically composed of (non-adhesive) hydrogel, maintains the shape of the printed construct until postprinting structure formation has taken place, at which point it is removed (figures 2(*C*)–(*H*)). Thus, it is not a part of the engineered construct.

The bioprinter is a mechanical extruder (NovoGen MMX Bioprinter^{TM}; Organovo, Inc., San Diego, CA; figure 2(*B*)) that enables the fabrication of three-dimensional tissue constructs in a wide variety of geometries. The platform is compatible with many soft tissue cell types and hydrogels. One of the two dispense pumps (figure 2(*B*)) prints cellular material, and the other hydrogels (used in particular to construct the temporary support structure). The dispense heads accommodate the special-purpose micropipette cartridges with diameters typically between 250–500 μm. Cellular aggregates can be deposited either in a cylindrical or spherical shape. The unit fits within a standard biosafety cabinet for sterile operation. The printer includes an intuitive software program with two modes of operation. Users can either select a stored design template (figures 2(*D*)–(*H*)), such as tubes (figures 2(*E*), (*F*) and (*H*)) or create a custom program. User-defined parameters enable the printing of more complex shapes such as branched tubular structures (figure 2(*G*)) or networked sheets.

2.3. Structure formation

Deposition of the bioink is the first step towards building tissue and organ substitutes. The role of the mechanical printer is the rapid and accurate arrangement of the cellular material. Biological structures form post-printing through shape forming processes akin to those of early embryonic morphogenesis, such as tissue fusion (figure 2(*D*)) and cell sorting [59]. Once fusion and preliminary sorting have taken place the engineered construct is transferred into a bioreactor, which provides near physiological conditions and where further maturation takes place (figure 3). In the case of vascular grafts the bioreactor provides pulsatile flow and the maturing graft develops biomechanical properties (such as burst pressure, contractility, suture retention strength) necessary for implantation.

The biophysical basis of post-printing structure formation is tissue liquidity [60], the notion that tissues composed of motile and adhesive cells have apparent liquid properties. Indeed, in suspensions or on non-adhesive surfaces, multicellular aggregates round up as liquid droplets (this property allows the formation of spherical bioink units). Cells of two distinct tissues randomly intermixed within such aggregates sort into separate regions similar to immiscible liquids (e.g. endothelial cells sort to the periphery of a developing vascular graft [45]). Two multicellular aggregates fuse similar to liquid drops (this property underlies the notion of bioink and gives rise to post-printing continuous structures). If tissue and multicellular aggregates (i.e. bioink units) are analogous to liquids, they must possess apparent surface and interfacial tension and viscosity. Such properties have been measured in artificial multicellular aggregates as well as living tissues [61–67] and are shown to give an account of observed sorting patterns [63] and tissue positioning in early development [61, 67].

To account for the liquid-like behavior of cell populations and tissues that display it, Steinberg formulated the 'differential adhesion hypothesis' (DAH), that provides the molecular basis for the liquid–tissue analogy in terms of tissue affinities [60]. The validity of DAH has been demonstrated both *in vitro* [62–64] and *in vivo* [68–70]. Computer simulations and theoretical approaches applying the principles of the DAH and using specific models of liquids reproduce the equilibrium configurations that tissues attain in sorting and fusion experiments [71–74]. As the presented tissue engineering approach utilizes early developmental phenomena [44, 75], it is predicated on the recognition that 'nature knows best'.

3. Bioprinted vascular constructs

Cardiovascular disease (CVD) remains the leading cause of death in the United States [76]. While autologous vessels are the preferred source of bypass conduits, CVD patients often lack native vascular conduits suitable for surgical intervention. In addition, surgical harvesting of autologous

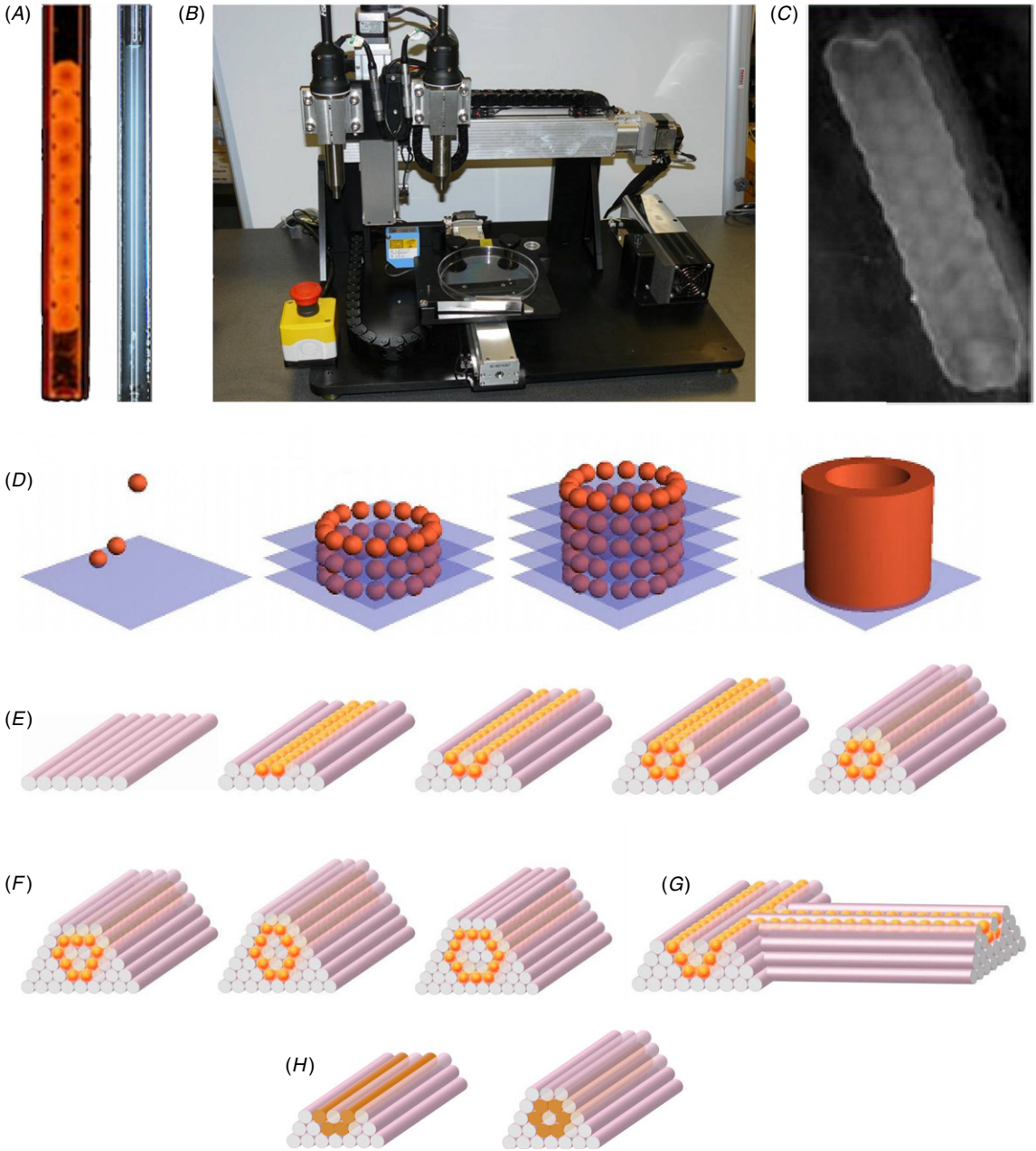

Figure 2. (*A*) Capillary micropipettes containing either contiguously arranged cellular aggregates (left) or cellular cylinders (right) as printer cartridges. (*B*) The Novogen MMX bioprinter™ (Organovo, San Diego, CA). It has two printing heads. One prints cellular material, the other cell-inert hydrogels. The stage of the apparatus houses a heated vial (to keep agarose in liquid form for aspiration into the micropipette), a cooled reservoir (to gel the content of the gel capillary) and a laser calibration device to calibrate the position of the micropipette. (*C*) Tubular construct printed using 500 μm cell aggregates. (*D*) and (*E*). Schematics to print tubular structures with cellular spheroids: layer-by-layer deposition of spheroids into the hydrogel (blue; *D*) or into a configuration supported by the cell-inert hydrogel rods (pink; *E*). (*F*) Templates to print tubes of varying diameter. (*G*) Template to build a branching tubular structure with the spheroid bioink. (*H*) Template to print tubes with the cylindrical bioink. (Panels *E, F* and *H* reproduced from [58].)

vascular conduits may result in post-operative complications including delayed wound healing, compromised regional blood flow and infection [77]. As native or natural vascular tissue for bypass grafting is limited, synthetic materials have been successfully used for large diameter, high-flow grafts. These however fail when the inner diameter (ID) is less than 6 mm (e.g. due to thrombogenicity and compliance mismatch) [78, 79]. Use of synthetic grafts often results in infection, leading to longer post-operative hospital stays and increased treatment costs [79].

Tissue engineering offers alternatives to current clinical options for CVD patients and other pathological conditions [10, 80–85]. The traditional approach here too is based on scaffolds [86]. The strategy for engineering small diameter conduits is to employ synthetic or natural tubular scaffolds seeded with vascular cells ([87, 88]). However, limitations of scaffold-based approaches have resulted in grafts with

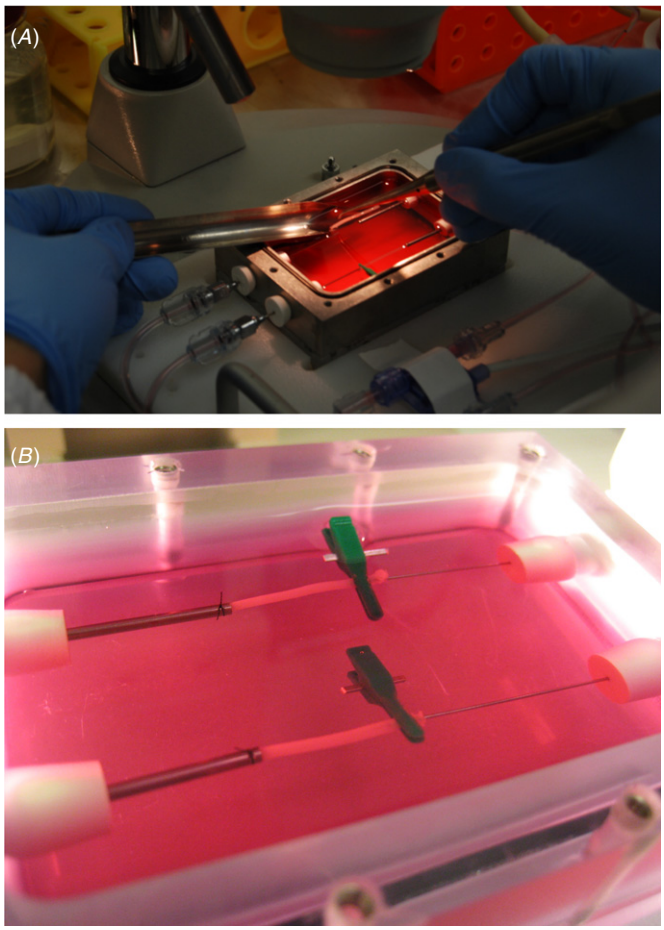

Figure 3. Bioreactor for post-printed maturation of bioprinted vessels. (*A*) Transfer of a vessel to a custom-built bioreactor. (*B*) Cannulating the vessels (see the text). The direction of the applied flow through the vessels is from right to left. Panel *B* reproduced from [58].

poor mechanical properties. In addition, remnants of the degrading scaffold may interfere with normal tissue maturation and lead to inflammation and mechanical failure [89]. Here we overview the construction of scaffold-free bioprinted vascular constructs comprised of vascular smooth muscle cells, endothelial cells and dermal fibroblasts.

3.1. Bioink for vascular constructs

Tubular vascular constructs can be fabricated with cylindrical bioink units (prepared as described in section 2.1 and in previous reports [56, 58, 90]) composed of aortic smooth muscle cells (HASMC), human aortic endothelial cells (HAEC) and human dermal fibroblasts (HDFb) mixed in appropriate ratios.

3.2. Building the vascular graft

Vascular conduits are constructed by co-printing the cylindrical bioink with cell-inert NovoGel^{TM} (Organovo Inc., San Diego, USA) rods, according to design templates shown schematically in figure 2. By adjusting the number of central NovoGel rods (figure 2(*F*)), the diameter of the engineered

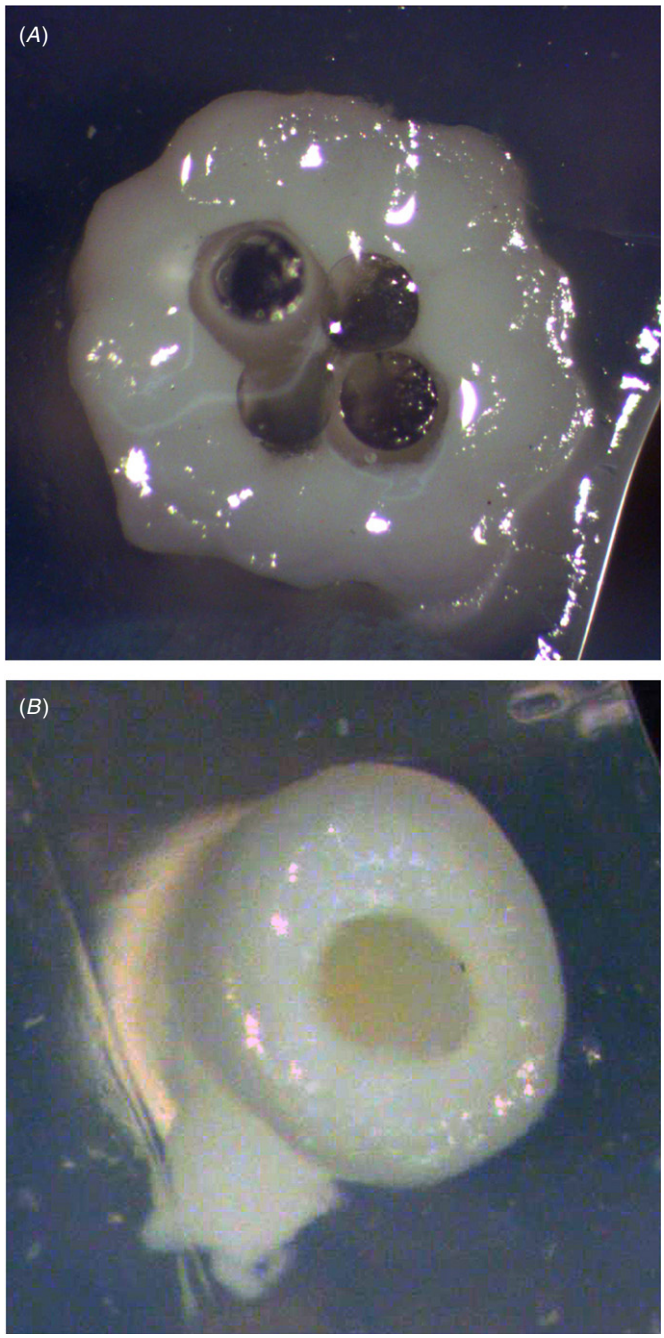

Figure 4. (*A*) Cross-section of a vascular graft printed with four central NovoGel rods 12 h post- printing. All cellular cylinders have fused to form a continuous conduit. (*B*) A vascular construct (ID = 600 μm), with NovoGel removed and fixed for histology, at 14 days post-perfusion.

vascular constructs can be altered (e.g. using 300 μm cylinders, the final vascular structure, in figure 2(*F*) rightmost panel has an ID of about 900 μm and a wall thickness of 300 μm). Post-printing, the construct is incubated for ~6 h to ensure fusion of neighboring cellular cylinders (figure 4(*A*)), at which point the surrounding and central hydrogel material is removed, yielding a vascular graft containing only cells and cell-produced ECM. Subsequently, the cellular construct is perfused in an appropriate bioreactor for vessel conditioning and maturation (figure 3(*A*)). Vessels are cannulated with

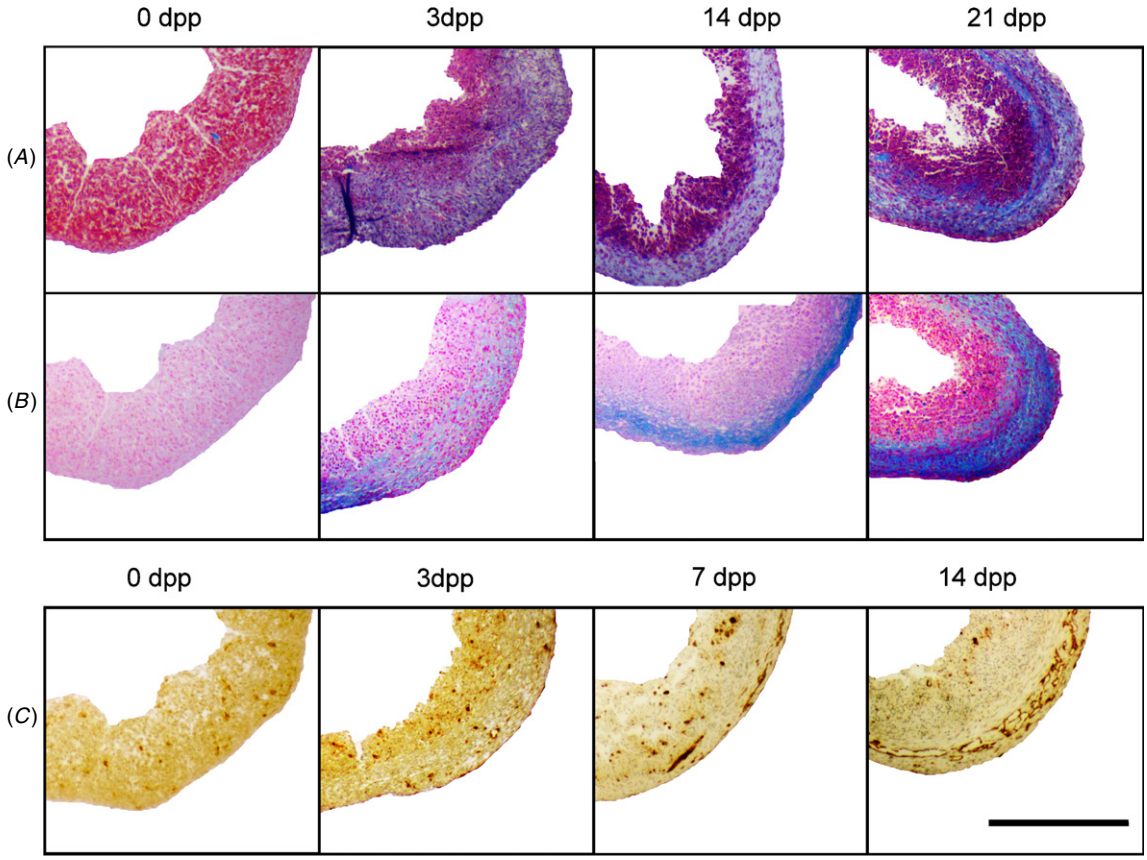

Figure 5. Histological analysis of bioprinted vascular grafts of three cell types (HASMC, HAEC, HDFb in a 70:25:5 ratio). (*A*) Massons trichrome staining of histological sections at specific time points in days post-perfusion (dpp) in the bioreactor, as indicated. Collagen stains blue and cytoplasm red. (*B*) Alcian blue staining of histological sections at specific dpp. Mucopolysaccharides and glycosaminoglycans stain blue and cytoplasm pink (*C*). CD31 staining of histological sections at specific dpp as indicated. CD31 positive endothelial cells stain dark brown. Day 0 refers to the time immediately post-fusion. Scale bar: 500 μm for all panels.

a blunt-tipped needle at the proximal end to the perfusing medium (for inner diameter of approximately 0.9 mm, 21G needles are used) and secured with microvascular clamps. The distal end is inserted into a larger needle (14G for the above conditions) with two sets of opposing holes bored in the tip, and secured in place (with 8–0 suture; figure 3(*B*)).

Perfusion of the post-fusion vessel is initially of very low flow rate, as no significant ECM has been produced at this point and the construct is capable of withstanding only low pressure (6 to 12 mmHg). Adjusting the flow conditions (laminar versus pulsatile) allows exposing the maturing vessel also to appropriate biomechanical stimuli. At specific time intervals constructs are fixed through the proximal cannula (with either formalin in 10% neutral buffer or 4% paraformaldehyde; figure 4(*B*)). Fixed vessels are prepared for histology and immunohistochemistry. As presented here, fused cellular vascular constructs were perfused in bioreactor chambers up to 21 days.

3.3. Structural properties of post-printed vascular grafts

Perfusion in the bioreactor stimulates the synthesis of ECM proteins. Trichrome staining of tissue sections reveals the extensive collagenous ECM as early as 3 days post-perfusion and demonstrates increased organization within the vessel wall over 21 days (figure 5(*A*)). Alcian blue staining reveals a similar trend for production and organization of glycosaminoglycans (GAGs; figure 5(*B*)).

Bioprinted vascular constructs were fabricated using mixtures of HASMC, HDFb and HAEC. DAH predicts that the HAEC will sort to the periphery of spherical [91] or cylindrical structures [44] containing both the HAEC and HASMC. It is less clear, however, how the presence of dermal fibroblasts in this system would affect the behavior of the HASMC and HAEC within the context of the DAH model. Bioink cylinders prepared with the three distinct cell types were successfully printed into tubular vascular constructs. CD31 immunostaining was performed to assess the location of the HAEC within the vessel wall (figure 5(*C*)). Initially (i.e. day 0), the HAEC were uniformly distributed throughout. Interestingly, within 3 days post-perfusion, the HAEC started to aggregate toward the periphery, and within two weeks of perfusion formed networks that mimic the *vaso-vasorum* of native vessels (figure 5(*C*)).

While we hypothesized that the HAEC would sort to the lumen of the vascular constructs and form a continuous endothelium (intima), our data do not support this hypothesis. However, when instead of the HAEC, human umbilical endothelial cells were used, those did sort to the lumen [45]. Thus a possible reason for the results presented here is that the

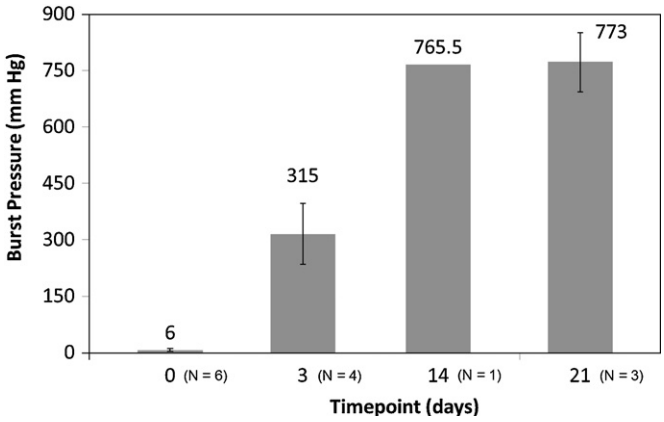

Figure 6. Burst pressures of vascular grafts (composed of HASMC, HAEC, HDFb in a 70:25:5 ratio) at specific time points post-perfusion. Values above the bars represent mean values for *N* samples as indicated next to individual time points. Data represent mean ± SD.

cells used (i.e. HASMC and HAEC) have a different source (i.e. do not originate from the same patient). A further possible explanation is that HAEC initially sort to both the inner and outer peripheries, but those at the lumen are sheared from the vessel wall upon the removal of the central hydrogel cylinders. It is also possible that the HAEC–HASMC interaction near the lumen is initially weak and even extremely low perfusion rates are sufficient to strip the lumen of the provisional intima. Finally, while the generation of bioink cylinders, containing the three vascular cell types confers specific advantages (i.e. increased cylinder strength, decreased cylinder shortening), sorting of cell populations within the cylinders may not occur as predicted by DAH [92, 93], at least not for the cell ratios used. Accordingly, it may be necessary to pursue alternative strategies for endothelialization.

3.4. Mechanical properties of post-printed vascular grafts

At specific time points post-perfusion, vascular constructs were subjected to a burst pressure test (figure 6). Not surprisingly, in the absence of any ECM immediately post-fusion (i.e. day 0) the bioprinted constructs burst at a minimal value of 6 mm Hg. However, burst pressure values increased with production and organization of the ECM. Bioprinted vascular constructs burst at 315 ± 81 mm Hg at 3d, and 773 ± 78 mm Hg at 21d.

4. Bioprinted nerve graft

The described bioprinting technology has also been used to fabricate fully biological nerve grafts for repair of peripheral nerve injury. Peripheral nerves do not heal as well as other tissues and regeneration of motor and/or sensory functions decrease rapidly with the extent of the wound leading to disability and chronic pain. Clinically, the best repair option is to replace the missing segment with an autologous graft [94]. Unfortunately, autografting has many shortcomings (e.g. limited availability of donor tissue, sacrifice of one or more functioning nerves, possible morbidity at the donor site).

Nerve grafting with other tissues has been used as an alternative. Autologous vein grafts promote axon regeneration and nerve conductivity at a level similar to autologous nerve grafts in a rat model [95]. Clinically, return of function was obtained on repairs smaller than 3 cm [96]. Due to constriction by surrounding scar tissue, for larger gaps, the use of vein grafts was compromised [97]. Such collapse was reduced by addition of nerve slices [98] or fresh muscle [99] inside the vein graft. Muscle was considered as a good candidate because of the longitudinal orientation of the fibers that could serve as axon guides (reviewed in [100]). However, the clinical application of vein, muscle or mixed grafts has been limited as these techniques are only efficient for small gaps and necessitate obtaining tissues from the patient. In this respect, allografts are more attractive but require immunosuppression [101]. An option to limit immune problems is to use decellularized tissues. Experiments in rats showed that grafts derived from acellular muscle and acellular nerve achieved similar regeneration to autologous grafts albeit with a delayed initiation phase [102]. Clinically, improved regeneration (up to 5 cm) has been obtained with decellularized allograft nerves recovered from cadaveric donors (Advance, AxoGen Inc.; FDA approved in 2007; http://www.axogeninc.com/products.html).

Tissues rich in ECM polymers (e.g. collagen, laminin) have been engineered into implantable nerve graft. For examples, amniotic membrane rolled around a mandrel to form a hollow tube produced results close to nerve autograft in a 1 cm rat model [103, 104]. Satisfying regeneration was also observed in rats implanted with small intestine submucosa layer seeded with Schwann cells (SC) and rolled into a cylinder [105]. Another way to obtain sheets is to have cells form them. This approach was used to fabricate a fully biological graft composed of a self-organized layer of rat fibroblasts seeded with fetal rat nerve cells [36]. As the fibroblasts produce collagen, they also contract and the cellular sheet rolls into a cylinder with conductive properties due to the network of nerve cells. However, the translation of such a construct to the clinic could be impaired by cell sources. Fibroblasts can easily be obtained from the patient but the fetal nerve cells would have to be substituted. On the other hand, a scaffoldless method is attractive since the construct is fully biocompatible.

Despite intense efforts to engineer an artificial 'off-the-shelf' nerve graft only a few synthetic (Neurotube, http://www.synovismicro.com/gem_neurotube.php; Neurolac http://www.polyganics.com/peripheral-nerve-repair/neurolac/neurolac.html) and natural (Avance, http://www.axogeninc.com/products.html; Integra, http://www.ilstraining.com/NTC%20Solutions/NeuraGen/NeuraGen_00.html; SaluBridge, http://www.salumedica.com/technology.htm) nerve guidance tubes have been approved for limited clinical use [106] (e.g. limited length gaps). Poor performance of nerve guidance conduits over larger distances has been linked to impaired axonal growth due to the conduits' limited physical properties (porosity, biodegradability, mechanical strength, inflammatory and immunological responses triggered by scaffold or its degradation products), insufficient infiltration of SC needed for a supportive environment to guide axons

and the lack of longitudinally oriented structural features mimicking endoneural architecture.

A tissue-engineered nerve graft, superior to autologous nerve grafts, has still to be built. Strategies to engineer such a graft should incorporate physical, molecular and biological elements [107]. The addition of supportive cells, in particular SC, into the lumen of the nerve guidance tube is a must and should be combined with any topographic or molecular improvement [108]. Since SC are hard to isolate and culture, alternative cell types have been considered (e.g. olfactory ensheathing cells [109], hair follicle stem cells [110], bone marrow stem cells [111]). Different options have been followed to enhance the topographic suitability of nerve guidance tubes. With the development of microfabrication techniques microtopographical patterns were created using synthetic materials. These are systematically being studied and modified to optimize for SC behavior (e.g. adhesion) and oriented neurite progression [112]. In particular, nanofibers had their physical parameters (diameter, porosity) tailored for use as nerve guidance tubes with luminal topography favorable to nerve regeneration [113, 114]. Some natural fibers such as spider silk have also been employed into nerve guidance tube [115]. Another strategy to enhance nerve guidance tube potential is to fill it with hydrogels (e.g. agarose, collagen, chitosan, hyaluronic acid, keratin) in association with ECM components (e.g. laminin, fibronectin, proteoglycans) and neurotrophic factors (e.g. nerve growth factor, fibroblast growth factor) to create a growth permissive environment for cells to add [116]. In what follows, we outline how the described bioprinting technology can be applied to fabricate fully biological nerve grafts and circumvent a number of issues discussed above.

4.1. Design and bioink

We designed a scaffold-free nerve graft guided by the following considerations: (i) the choice of a rat sciatic nerve injury model for implantation; (ii) the creation of a multi-lumen pattern to increase the luminal surface area available for support cells to favor axon regeneration; (iii) the cell type to support axon regeneration and to be suitable for cylindrical bioink preparation. Furthermore, the graft needed to have a diameter comparable to that of a rat sciatic nerve (∼2 mm) and be at least 1 cm long to fill the gap. Instructed by earlier results [117] 500 μm cylindrical bioink units were used (for their preparation see section 2.1).

As the density of supporting cells is a critical factor for axon regeneration [108], to establish proof of concept, initially a tube composed exclusively of SC was considered. Such tube was impossible to build because due to the lack of sufficient SC cell–cell adhesion, the cylindrical bioink particles were not sufficiently strong for printing. Hair follicles-derived stem cells and bone marrow stem cells (BMSC) have successfully been used as a source of support cells for nerve regeneration and trans-differentiation into SC [110, 118]. We observed that BMSC form adequate cylindrical bioink units. BMSC have also been shown to possess anti-inflammatory properties beneficial for tissue regeneration. Additionally, mesenchymal stem cells, a subcellular fraction of BMSC, can differentiate into Schwann-like cells when co-cultured with SC [119]. Thus we employed BMSC to prepare the bioink.

4.2. Building the graft

Bioink units composed of BMSC (90%) and SC (10%) were used to form the central part of the graft. The two types of cylindrical bioink units (i.e. BMSC and BMSC:SC) were printed together with agarose support rods, according to the template shown in figure 7(*A*). The post-printing fusion of the discrete bioink units resulted in a tubular structure with three axially arranged parallel acellular channels (figure 7(*B*)) lined with SC (figure 7(*C*)). After 7-day maturation, the agarose rods were removed and the resulting multichannel construct was ready for implantation to bridge a severed nerve.

4.3. Implantation and post-implantation procedures

We implanted the bioprinted nerve grafts into laboratory rats. A 1 cm stretch of the nerve was surgically isolated and resected. (Female Sprague Daley rats, ∼400 g, were anesthetized per Office of Lab Animal medicine dosing recommendations via an intraperitoneal route. Implantation was performed under sterile conditions. Following sedation, the left lateral thigh of the rat was shaved and the rat hind limb was prepped and draped. Skin incisions were made along the mid lateral thigh and the skin flaps elevated exposing the musculo-fascia. This was incised and the interval between the thigh musculature was split longitudinally exposing the sciatic nerve at and distal to its branching point.) The gap resulting from the resection of the 1 cm stretch was bridged with the bioprinted nerve tube and the free ends of the native sciatic nerve were intubulated into the nerve tube and sutured to it. (To secure the engineered nerve tube it was floated into a longitudinally cut collagen nerve guide, approximately 12–14 mm in length (Neurogen, Integra Life Sciences, Plainboro, NJ). The wound was then irrigated, the muscle and skin closed (absorbable suture were used). Animals were let to recover on a warming pad in an isolated cage.

Implanted grafts were harvested after three weeks (using a surgical procedure similar to the one for implantation) with the proximal and distal nerve stumps and photographed for morphological observations. Tissues were fixed (overnight in 4% paraformaldehyde) and prepared for histological assessments (i.e. dehydrated with an ethanol series, sectioned and processed for paraffin infiltration and embedding).

Axons visibly reached the distal segment of the sciatic nerve in all the histological sections taken along the repair (data not shown). Manual counting showed that about 40% of the axons present in the proximal stump crossed the bioengineered nerve graft and reached the distal stump (figure 8). Encouraged by the extent of regeneration and the biocompatibility of the bioprinted nerve grafts, a more exhaustive study is underway to compare their functional properties with those of autologous grafts.

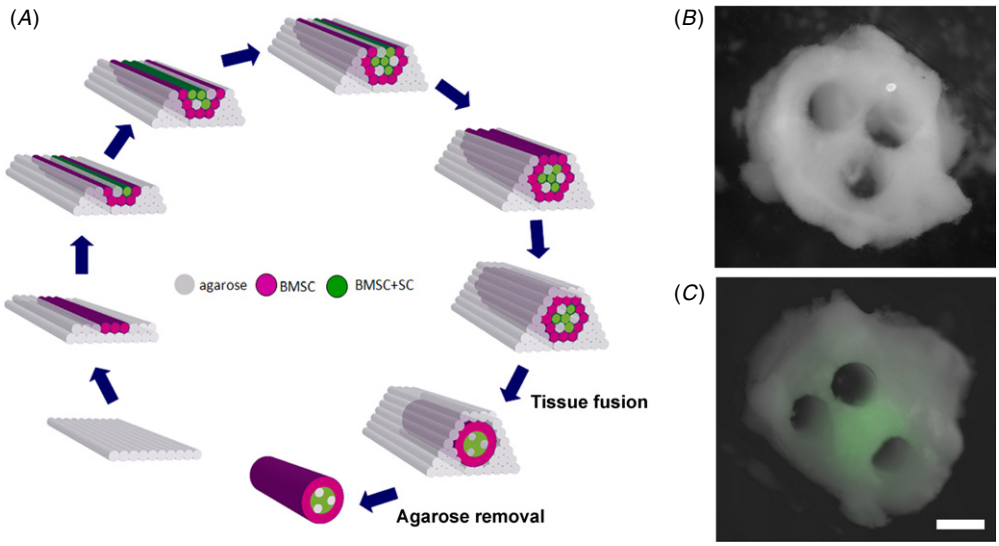

Figure 7. (*A*) Possible scheme for deposition of cellular (red: BMSC, green: 90% BMSC + 10% SC) and agarose cylinders (gray) to build a 3-lumen tube. (*B*) Cross-section of a bioprinted nerve graft, constructed according to the scheme in A, with three acellular channels. (*C*) Fluorescently labeled Schwann cells (green) concentrated at the central region of the graft. Scale bar: 500 μm.

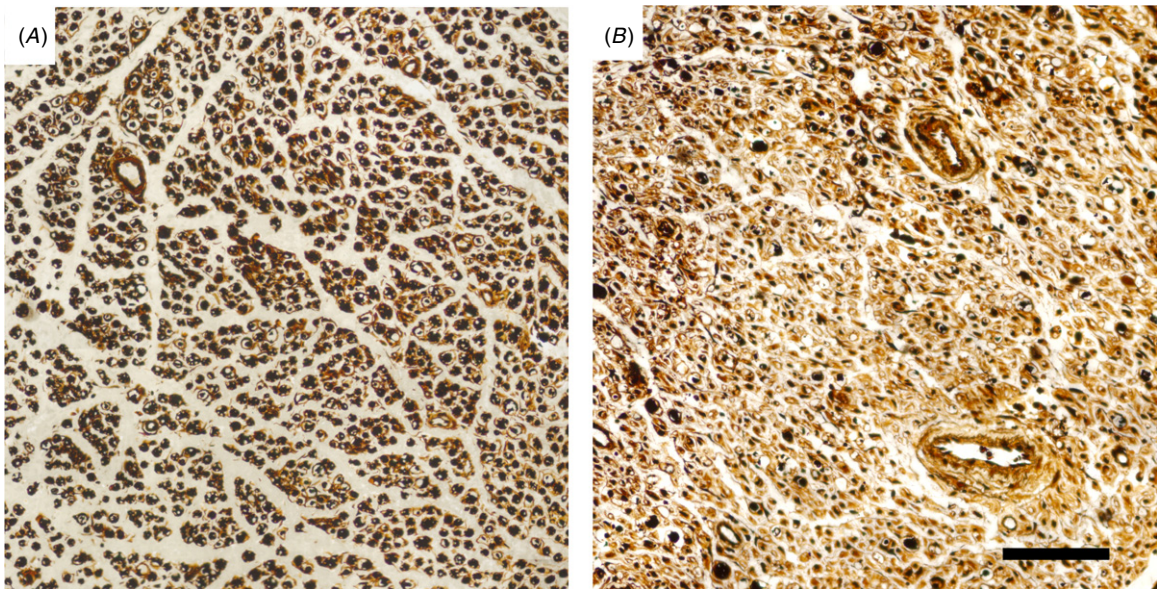

Figure 8. Partial view of proximal (*A*) and distal (*B*) transverse, 4 mm sections within the bioprinted nerve graft wrapped in a collagen tube after three weeks of repair. For global aspect, sections were stained with hematoxylin–eosin. To detect axons (black dots), Bielschowsky staining was performed. Scale bar: 100 μm.

5. Concluding remarks

Tissue engineering traditionally uses cells, scaffolds and bioreactors to build replacement tissues. Here we overviewed a scaffold-free, self-assembly-based method that employs bioprinting to construct three-dimensional tissue and organ structures with desired functional and topological properties. The process consists of (1) pre-processing, (2) processing and (3) post-processing phases. In the preparatory phase 1, the discrete multicellular bioink units, with tissue or organ specific composition are prepared and packaged into printer cartridges. In phase 2 the discrete bioink units are delivered by the bioprinter into a supporting environment, according to a design template chosen according to the architectural features of the desired structure. It is in phase 3, where the continuous biological structure forms by mechanisms akin to those acting in early morphogenesis, such as tissue fusion and sorting. Immediately post-printing the biological structure has not yet developed its own tissue or organ-specific ECM. Thus it is further matured in the bioreactor that provides near-physiological conditions to achieve the necessary biomechanical and biochemical conditions for eventual implantation.

We illustrated the technology by applying it to build fully biological vascular and nerve grafts. These structures can be clinically relevant on their own, or serve as building blocks for more complex structures. For example, engineered vascular grafts make it possible to fabricate vascularized

tissues, a major challenge for tissue and organ engineering at present. Due to its versatility it is to be expected that the technology will have many other applications. Besides obvious ones, such as resource for three-dimensional tissue culture or providing truly three-dimensional biological constructs for basic research in developmental biology, it is likely to be employed by the pharmaceutical industry. Rapidly and reproducibly prepared three-dimensional functional biological constructs of specific topology, built of human cells, could serve as tissue intermediates between animal and human clinical trials for drug testing. Such application may lead to significant savings in the ubiquitously high cost of drug development.

Acknowledgments

This research was partially supported by NSF (grant EF0256854) and by the University of Missouri Research Board.

References

[1] Lanza R P, Langer R S and Vacanti J 2007 *Principles of Tissue Engineering* (Burlington, MA: Elsevier)
[2] Hollander A P and Hatton P V (ed) 2010 *Biopolymer Methods in Tissue Engineering* (Totowa, NJ: Humana Press)
[3] Kasper C, Van Griensven M and Pörtner R (ed) 2009 *Bioreactor Systems for Tissue Engineering* (Berlin: Springer)
[4] Grayson W L, Chao P H, Marolt D, Kaplan D L and Vunjak-Novakovic G 2008 Engineering custom-designed osteochondral tissue grafts *Trends Biotechnol.* **26** 181–9
[5] Mikos A G *et al* 2006 Engineering complex tissues *Tissue Eng.* **12** 3307–39
[6] Radisic M *et al* 2004 Functional assembly of engineered myocardium by electrical stimulation of cardiac myocytes cultured on scaffolds *Proc. Natl Acad. Sci. USA* **101** 18129–34
[7] Tandon N *et al* 2009 Electrical stimulation systems for cardiac tissue engineering *Nature Protoc.* **4** 155–73
[8] Vunjak-Novakovic G, Altman G, Horan R and Kaplan D L 2004 Tissue engineering of ligaments *Annu. Rev. Biomed. Eng.* **6** 131–56
[9] Fischbach C and Mooney D J 2007 Polymers for pro- and anti-angiogenic therapy *Biomaterials* **28** 2069–76
[10] Griffith L and Naughton G 2002 Tissue engineering—current challenges and expanding opportunities *Science* **295** 1009–14
[11] Atala A, Bauer S B, Soker S, Yoo J J and Retik A B 2006 Tissue-engineered autologous bladders for patients needing cystoplasty *Lancet* **367** 1241–6
[12] Niklason L E *et al* 1999 Functional arteries grown *in vitro* *Science* **284** 489–93
[13] Hibino N *et al* 2010 Late-term results of tissue-engineered vascular grafts in humans *J. Thorac. Cardiovasc. Surg.* **139** 431–6
[14] Matsumura G *et al* 2006 Evaluation of tissue-engineered vascular autografts *Tissue Eng.* **12** 3075–83
[15] Oberpenning F, Meng J, Yoo J J and Atala A 1999 De novo reconstitution of a functional mammalian urinary bladder by tissue engineering *Nature Biotechnol.* **17** 149–55
[16] Raya-Rivera A *et al* 2011 Tissue-engineered autologous urethras for patients who need reconstruction: an observational study *Lancet* **377** 1175–82
[17] Shin'Oka T, Imai Y and Ikada Y 2001 Transplantation of a tissue-engineered pulmonary artery *N. Eng. J. Med.* **344** 532–3
[18] Shin'oka T *et al* 2005 Midterm clinical result of tissue-engineered vascular autografts seeded with autologous bone marrow cells *J. Thorac. Cardiovasc. Surg.* **129** 1330–8
[19] Badylak S F 2002 The extracellular matrix as a scaffold for tissue reconstruction *Semin. Cell. Dev. Biol.* **13** 377–83
[20] Gilbert T W, Sellaro T L and Badylak S F 2006 Decellularization of tissues and organs *Biomaterials* **27** 3675–83
[21] Hoshiba T, Lu H, Kawazoe N and Chen G 2010 Decellularized matrices for tissue engineering *Expert Opin. Biol. Ther.* **10** 1717–28
[22] Baiguera S *et al* 2010 Tissue engineered human tracheas for *in vivo* implantation *Biomaterials* **31** 8931–8
[23] Dahl S L M, Koh J, Prabhakar V and Niklason L E 2003 Decellularized native and engineered arterial scaffolds for transplantation *Cell Transplant.* **12** 659–66
[24] Gui L, Muto A, Chan S A, Breuer C K and Niklason L E 2009 Development of decellularized human umbilical arteries as small-diameter vascular grafts *Tissue Eng.* A **15** 2665–76
[25] Murase Y *et al* 2006 Evaluation of compliance and stiffness of decellularized tissues as scaffolds for tissue-engineered small caliber vascular grafts using intravascular ultrasound *ASAIO J.* **52** 450–5
[26] Petersen T H, Calle E A, Colehour M B and Niklason L E 2011 Matrix composition and mechanics of decellularized lung scaffolds *Cells Tissues Organs* in press
[27] Ponce Marquez S *et al* 2009 Decellularization of bovine corneas for tissue engineering applications *Acta Biomater.* **5** 1839–47
[28] Prasertsung I, Kanokpanont S, Bunaprasert T, Thanakit V and Damrongsakkul S 2008 Development of acellular dermis from porcine skin using periodic pressurized technique *J. Biomed. Mater. Res.* B **85** 210–9
[29] Ross E A *et al* 2009 Embryonic stem cells proliferate and differentiate when seeded into kidney scaffolds *J. Am. Soc. Nephrol.* **20** 2338–47
[30] Zeltinger J, Landeen L K, Alexander H G, Kidd I D and Sibanda B 2001 Development and characterization of tissue-engineered aortic valves *Tissue Eng.* **7** 9–22
[31] Godier-Furnemont A F *et al* 2011 Composite scaffold provides a cell delivery platform for cardiovascular repair *Proc. Natl Acad. Sci. USA* **108** 7974–9
[32] Dahl S L *et al* 2011 Readily available tissue-engineered vascular grafts *Sci. Transl. Med.* **3** 68ra69
[33] Ott H C *et al* 2008 Perfusion-decellularized matrix: using nature's platform to engineer a bioartificial heart *Nature Med.* **14** 213–21
[34] Baptista P M *et al* 2011 The use of whole organ decellularization for the generation of a vascularized liver organoid *Hepatology* **53** 604–17
[35] Macchiarini P *et al* 2008 Clinical transplantation of a tissue-engineered airway *Lancet* **372** 2023–30
[36] Baltich J, Hatch-Vallier L, Adams A M, Arruda E M and Larkin L M 2010 Development of a scaffoldless three-dimensional engineered nerve using a nerve-fibroblast co-culture *In Vitro Cell. Dev. Biol. Anim.* **46** 438–44
[37] L'Heureux N *et al* 2006 Human tissue-engineered blood vessels for adult arterial revascularization *Nature Med.* **12** 361–5

[38] L'Heureux N *et al* 2007 Technology insight: the evolution of tissue-engineered vascular grafts—from research to clinical practice *Nature Clin. Pract. Cardiovasc. Med.* **4** 389–95

[39] L'Heureux N, McAllister T N and de la Fuente L M 2007 Tissue-engineered blood vessel for adult arterial revascularization *N. Eng. J. Med.* **357** 1451–3

[40] McAllister T N *et al* 2009 Effectiveness of haemodialysis access with an autologous tissue-engineered vascular graft: a multicentre cohort study *Lancet* **373** 1440–6

[41] Tsuda Y *et al* 2007 Cellular control of tissue architectures using a three-dimensional tissue fabrication technique *Biomaterials* **28** 4939–46

[42] Hannachi I, Yamato M and Okano T 2009 Cell sheet technology and cell patterning for biofabrication *Biofabrication* **1** 022002

[43] Jakab K, Neagu A, Mironov V, Markwald R R and Forgacs G 2004 Engineering biological structures of prescribed shaped using self-assembling multicellular systems *Proc. Natl Acad. Sci. USA* **101** 2864–9

[44] Jakab K *et al* 2010 Tissue engineering by self-assembly and bio-printing of living cells *Biofabrication* **2** 022001

[45] Mironov V, Boland T, Trusk T, Forgacs G and Markwald R R 2003 Organ printing: computer-aided jet-based 3D tissue engineering *Trends Biotechnol.* **21** 157–61

[46] Boland T, Xu T, Damon B and Cui X 2006 Application of inkjet printing to tissue engineering *Biotechnol. J.* **1** 910–7

[47] Campbell P G and Weiss L E 2007 Tissue engineering with the aid of inkjet printers *Expert Opin. Biol. Ther.* **7** 1123–7

[48] Cui X, Dean D, Ruggeri Z M and Boland T 2010 Cell damage evaluation of thermal inkjet printed Chinese hamster ovary cells *Biotechnol. Bioeng.* **106** 963–9

[49] Nakamura M *et al* 2005 Biocompatible inkjet printing technique for designed seeding of individual living cells *Tissue Eng.* **11** 1658–66

[50] Roth E A *et al* 2004 Inkjet printing for high-throughput cell patterning *Biomaterials* **25** 3707–15

[51] Chang R, Nam J and Sun W 2008 Effects of dispensing pressure and nozzle diameter on cell survival from solid freeform fabrication-based direct cell writing *Tissue Eng.* A **14** 41–8

[52] Barron J A, Bradley R R, Kim H, Spargo B J and Chrisey D B 2004 Application of laser printing to mammalian cells *Thin Solid Films* **453–454** 383–7

[53] Catros S *et al* 2011 Laser-assisted bioprinting for creating on-demand patterns of human osteoprogenitor cells and nano-hydroxyapatite *Biofabrication* **3** 025001

[54] Odde D J and Renn M J 1999 Laser-guided direct writing for applications in biotechnology *Trends Biotechnol.* **17** 385–9

[55] Cohen D L, Malone E, Lipson H and Bonassar L J 2006 Direct freeform fabrication of seeded hydrogels in arbitrary geometries *Tissue Eng.* **12** 1325–35

[56] Jakab K, Damon B, Neagu A, Kachurin A and Forgacs G 2006 Three-dimensional tissue constructs built by bioprinting *Biorheology* **43** 509–13

[57] Lin R Z and Chang H Y 2008 Recent advances in three-dimensional multicellular spheroid culture for biomedical research *Biotechnol. J.* **3** 1172–84

[58] Norotte C, Marga F S, Niklason L E and Forgacs G 2009 Scaffold-free vascular tissue engineering using bioprinting *Biomaterials* **30** 5910–7

[59] Perez-Pomares J M and Foty R A 2006 Tissue fusion and cell sorting in embryonic development and disease: biomedical implications *Bioessays* **28** 809–21

[60] Steinberg M S 1963 Reconstruction of tissues by dissociated cells. Some morphogenetic tissue movements and the sorting out of embryonic cells may have a common explanation *Science* **141** 401–8

[61] Damon B J, Mezentseva N V, Kumaratilake J S, Forgacs G and Newman S A 2008 Limb bud and flank mesoderm have distinct 'physical phenotypes' that may contribute to limb budding *Dev. Biol.* **321** 319–30

[62] Forgacs G, Foty R A, Shafrir Y and Steinberg M S 1998 Viscoelastic properties of living embryonic tissues: a quantitative study *Biophys. J.* **74** 2227–34

[63] Foty R A, Pfleger C M, Forgacs G and Steinberg M S 1996 Surface tensions of embryonic tissues predict their mutual envelopment behavior *Development* **122** 1611–20

[64] Hegedus B, Marga F, Jakab K, Sharpe-Timms K L and Forgacs G 2006 The interplay of cell-cell and cell-matrix interactions in the invasive properties of brain tumors *Biophys. J.* **91** 2708–16

[65] Jakab K *et al* 2008 Relating cell and tissue mechanics: implications and applications *Dev. Dyn.* **237** 2438–49

[66] Norotte C, Marga F, Neagu A, Kosztin I and Forgacs G 2008 Experimental evaluation of apparent tissue surface tension based on the exact solution of the Laplace equation *Europhys. Lett.* **81** 46003

[67] Schötz E *et al* 2008 Quantitative differences in tissue surface tension influence zebrafish germ layer positioning *HFSP* **2** 42–56

[68] Godt D and Tepass U 1998 Drosophila oocyte localization is mediated by differential cadherin- based adhesion *Nature* **395** 387–91

[69] Gonzalez-Reyes A and St Johnston D 1998 Patterning of the follicle cell epithelium along the anterior-posterior axis during Drosophila oogenesis *Development* **125** 2837–46

[70] Hayashi T and Carthew R W 2004 Surface mechanics mediate pattern formation in the developing retina *Nature* **431** 647–52

[71] Glazier J A and Graner F 1993 Simulation of the differential adhesion driven rearrangement of biological cells *Phys. Rev.* E **47** 2128–54

[72] Gordon R, Goel N S, Steinberg M S and Wiseman L L 1972 A rheological mechanism sufficient to explain the kinetics of cell sorting *J. Theor. Biol.* **37** 43–73

[73] Marmottant P *et al* 2009 The role of fluctuations and stress on the effective viscosity of cell aggregates *Proc. Natl Acad. Sci. USA* **106** 17271–5

[74] Mombach J C, Glazier J A, Raphael R C and Zajac M 1995 Quantitative comparison between differential adhesion models and cell sorting in the presence and absence of fluctuations *Phys. Rev. Lett.* **75** 2244–7

[75] Forgacs G and Newman S 2005 *Biological Physics of the Developing Embryo* (Cambridge: Cambridge University Press)

[76] Thom T *et al* 2006 Heart disease and stroke statistics—2006 update: a report from the American Heart Association Statistics Committee and Stroke Statistics Subcommittee *Circulation* **113** e85–151

[77] Fowler V G Jr *et al* 2005 Clinical predictors of major infections after cardiac surgery *Circulation* **112** I358–65

[78] Edelman E R 1999 Vascular tissue engineering: designer arteries *Circ. Res.* **85** 1115–7

[79] Niklason L E and Langer R S 1997 Advances in tissue engineering of blood vessels and other tissues *Transpl. Immunol.* **5** 303–6

[80] Bonassar L J and Vacanti C A 1998 Tissue engineering: the first decade and beyond *J. Cell. Biochem. Suppl.* **30–31** 297–303

[81] Khademhosseini A, Langer R, Borenstein J and Vacanti J P 2006 Microscale technologies for tissue engineering and biology *Proc. Natl Acad. Sci. USA* **103** 2480–7

[82] Langer R 2000 Biomaterials in drug delivery and tissue engineering: one laboratory's experience *Acc. Chem. Res.* **33** 94–101

[83] Langer R and Vacanti J P 1993 Tissue engineering *Science* **260** 920–6

[84] Lysaght M J, Nguy N A and Sullivan K 1998 An economic survey of the emerging tissue engineering industry *Tissue Eng.* **4** 231–8

[85] Vacanti J P, Langer R, Upton J and Marler J J 1998 Transplantation of cells in matrices for tissue regeneration *Adv. Drug Deliv. Rev.* **33** 165–82

[86] Mironov V *et al* 2006 Cardiovascular tissue engineering: I. Perfusion bioreactors: a review *J. Long Term Eff. Med. Implants* **16** 111–30

[87] Isenberg B C, Williams C and Tranquillo R T 2006 Small-diameter artificial arteries engineered *in vitro Circ. Res.* **98** 25–35

[88] Kakisis J D, Liapis C D, Breuer C and Sumpio B E 2005 Artificial blood vessel: the Holy Grail of peripheral vascular surgery *J. Vasc. Surg.* **41** 349–54

[89] Dahl S L, Rhim C, Song Y C and Niklason L E 2007 Mechanical properties and compositions of tissue engineered and native arteries *Ann. Biomed. Eng.* **35** 348–55

[90] Jakab K *et al* 2008 Tissue engineering by self-assembly of cells printed into topologically defined structures *Tissue Eng.* A **14** 413–21

[91] Korff T, Kimmina S, Martiny-Baron G and Augustin H G 2001 Blood vessel maturation in a three-dimensional spheroidal coculture model: direct contact with smooth muscle cells regulates endothelial cell quiescence and abrogates VEGF responsiveness *FASEB J.* **15** 447–57

[92] Krieg M *et al* 2008 Tensile forces govern germ-layer organization in zebrafish *Nature Cell. Biol.* **10** 429–36

[93] Manning M L, Foty R A, Steinberg M S and Schoetz E M 2010 Coaction of intercellular adhesion and cortical tension specifies tissue surface tension *Proc. Natl Acad. Sci. USA* **107** 12517–22

[94] Millesi H 1968 On the problem of overbridging defects of the peripheral nerves *Wien. Med. Wochenschr.* **118** 182–7

[95] Chiu D T *et al* 1988 Comparative electrophysiologic evaluation of nerve grafts and autogenous vein grafts as nerve conduits: an experimental study *J. Reconstr. Microsurg.* **4** 303–9

[96] Chiu D T and Strauch B 1990 A prospective clinical evaluation of autogenous vein grafts used as a nerve conduit for distal sensory nerve defects of 3 cm or less *Plast. Reconstr. Surg.* **86** 928–34

[97] Tang J B, Shi D and Zhou H 1995 Vein conduits for repair of nerves with a prolonged gap or in unfavourable conditions: an analysis of three failed cases *Microsurgery* **16** 133–7

[98] Tang J B, Gu Y Q and Song Y S 1993 Repair of digital nerve defect with autogenous vein graft during flexor tendon surgery in zone 2 *J. Hand. Surg. Br.* **18** 449–53

[99] Battiston B, Tos P, Cushway T R and Geuna S 2000 Nerve repair by means of vein filled with muscle grafts: I. Clinical results *Microsurgery* **20** 32–6

[100] Meek M F, Varejão A S and Geuna S 2004 Use of skeletal muscle tissue in peripheral nerve repair: review of the literature *Tissue Eng.* **10** 1027–36

[101] Moore A M, Ray W Z, Chenard K E, Tung T and Mackinnon S E 2009 Nerve allotransplantation as it pertains to composite tissue transplantation *Hand* **4** 239–44

[102] Kerns J M, Danielsen N, Zhao Q, Lundborg G and Kanje M 2003 A comparison of peripheral nerve regeneration in acellular muscle and nerve autografts *Scand. J. Plast. Reconstr. Surg. Hand. Surg.* **37** 193–200

[103] Mohammad J, Shenaq J, Rabinovsky E and Shenaq S 2000 Modulation of peripheral nerve regeneration: a tissue-engineering approach. The role of amnion tube nerve conduit across a 1 centimeter nerve gap *Plast. Reconstr. Surg.* **105** 660–6

[104] O'Neill A C *et al* 2009 Preparation and integration of human amnion nerve conduits using a light-activated technique *Plast. Reconstr. Surg.* **124** 428–37

[105] Hadlock T A, Sundback C A, Hunter D A, Vacanti J P and Cheney M L 2001 A new artificial nerve graft containing rolled Schwann cell monolayers *Microsurgery* **21** 96–101

[106] Meek M F and Coert J H 2008 US Food and Drug Administration/Conformit Europe-approved absorbable nerve conduits for clinical repair of peripheral and cranial nerves *Ann. Plast. Surg.* **60** 110–6

[107] de Ruiter G C, Malessy M J, Yaszemski M J, Windebank A J and Spinner R J 2009 Designing ideal conduits for peripheral nerve repair *Neurosurg. Focus* **26** E5

[108] Guenard V, Kleitman N, Morrissey T K, Bunge R P and Aebischer P 1992 Syngeneic Schwann cells derived from adult nerves seeded in semipermeable guidance channels enhance peripheral nerve regeneration *J. Neurosci.* **12** 3310–20

[109] Radtke C *et al* 2009 Transplantation of olfactory ensheathing cells enhances peripheral nerve regeneration after microsurgical nerve repair *Brain Res.* **1254** 10–7

[110] Hoffman R M 2006 The pluripotency of hair follicle stem cells *Cell Cycle* **5** 232–3

[111] Wang D *et al* 2008 Bridging small-gap peripheral nerve defects using acellular nerve allograft implanted with autologous bone marrow stromal cells in primates *Brain Res.* **1188** 44–53

[112] Hoffman-Kim D, Mitchel J A and Bellamkonda R V 2010 Topography, cell response, and nerve regeneration *Annu. Rev. Biomed. Eng.* **12** 203–31

[113] Cunha C, Panseri S and Antonini S 2011 Emerging nanotechnology approaches in tissue engineering for peripheral nerve regeneration *Nanomedicine* **7** 50–9

[114] Kim Y T, Haftel V K, Kumar S and Bellamkonda R V 2008 The role of aligned polymer fiber-based constructs in the bridging of long peripheral nerve gaps *Biomaterials* **29** 3117–27

[115] Allmeling C *et al* 2008 Spider silk fibres in artificial nerve constructs promote peripheral nerve regeneration *Cell Prolif.* **41** 408–20

[116] Steed M B, Mukhatyar V, Valmikinathan C and Bellamkonda R V 2011 Advances in bioengineered conduits for peripheral nerve regeneration *Atlas Oral Maxillofac. Surg. Clin. North Am.* **19** 119–30

[117] Hadlock T, Sundback C, Hunter D, Cheney M and Vacanti J P 2000 A polymer foam conduit seeded with Schwann cells promotes guided peripheral nerve regeneration *Tissue Eng.* **6** 119–27

[118] Yamakawa T *et al* 2007 Nerve regeneration promoted in a tube with vascularity containing bone marrow-derived cells *Cell Transplant.* **16** 811–22

[119] Krampera M *et al* 2007 Induction of neural-like differentiation in human mesenchymal stem cells derived from bone marrow, fat, spleen and thymus *Bone* **40** 382–90